Available at: http://publications.ictp.it IC/2010/049

United Nations Educational, Scientific and Cultural Organization
and
International Atomic Energy Agency

THE ABDUS SALAM INTERNATIONAL CENTRE FOR THEORETICAL PHYSICS

JOINT INVERSION OF SURFACE WAVES DISPERSION AND RECEIVER FUNCTION AT CUBA SEISMIC STATIONS

O'Leary González[1], Bladimir Moreno[1]
Centro Nacional de Investigaciones Sismológicas,
Calle 17, No. 61 e/ 4 y 6 Vista Alegre, Santiago de Cuba, Cuba
and
The Abdus Salam International Centre for Theoretical Physics, Trieste, Italy,

Fabio Romanelli and Giuliano F. Panza
Department of Geosciences, University of Trieste, Trieste, Italy
and
The Abdus Salam International Centre for Theoretical Physics, Trieste, Italy.

Abstract

Joint inversion of Rayleigh wave group velocity dispersion and receiver functions have been used to estimate the crust and upper mantle structure at eight seismic stations in Cuba. Receiver functions have been computed from teleseismic recordings of earthquakes at epicentral (angular) distances between 30° and 90° and Rayleigh wave group velocity dispersion have been taken from a surface-wave tomography study of the Caribbean area. The thickest crust (around 27 km) is found at Cascorro (CCC), Soroa (SOR), Moa (MOA) and Maisí (MAS) stations while the thinnest crust (around 18 km) is found at stations Río Carpintero (RCC) and Guantánamo Bay (GTBY), in the southeastern of Cuba; this result is in agreement with the southward gradual thinning of the crust revealed by previous studies. The inversion shows a crystalline crust with S-wave velocity between 2.9 km/s and 3.9 km/s and at the crust-mantle transition zone the shear wave velocity varies from 3.9 km/s and 4.3 km/s. The lithospheric thickness varies from 74 km, in the youngest lithosphere, to 200 km in the middle of the Cuban island. Evidences of a subducted slab possibly belonging to the Caribbean plate are present below the stations Las Mercedes (LMG), RCC and GTBY and a thicker slab is present below the SOR station.

MIRAMARE – TRIESTE

June 2010

[1] Regular Associate of ICTP.

Introduction

Earlier studies have identified two different active tectonic periods in the development of the crust in Cuba. During the first period (Jurassic-Middle Eocene), an island arc with continental crust was formed on an oceanic basement (Pushcharovskiy, 1979). In late Eocene-Quaternary the earlier formed nappe-fold complexes, as a whole, were subjected to different character of deformations expressed in rises and basins of the present topography, and consequently in the features of the facies and thicknesses of the Middle and Upper Cenozoic sediments (Makarov, 1986). Cuba contains Precambrian rocks and sedimentary rocks of Jurassic to Cretaceous age, characterized by large thrust and nappe structures, which are not present in the other islands of the northern Caribbean (Draper and Barros, 1994). Over most of its length, Cuba is the divide between extremely stable geologic conditions to the north and complex ones to the south. Much of the north coast of Cuba belongs to the Florida-Bahamas carbonate province and much of the southern part consists of metamorphosed sedimentary and acidic igneous rocks. In the middle, as a result of the contact between the Bahamas platform and the Cuban island arc, there is a relatively narrow, extremely folded and faulted belt which contains ultra-basic igneous rocks and many types of volcanics and volcanic-derived sediments (Pardo, 1975).

According to Bush and Shcherbakova (1986), the Cuban region consists of a tectonic junction of three dissimilar crustal blocks: (1) an autochthonous segment of the North America plate with continental crust; (2) a Cretaceous volcanic island arc with transitional crust and over thrust structure; and (3) an autochthonous fragment of a Paleocene volcanic island arc. Satellite photograph interpretation (Bush and Shcherbakova, 1986) has been used to refine the position of Cuba's "axial fault" (AF), which extends for more than 800 km along the entire island. Bush and Shcherbakova (1986) interpreted this "axial fault" as the southern boundary of the contact zone between the Cuban island arc and the Bahamas platform. Based on joint interpretation of gravity and seismic refraction data, they found drastic changes in the crustal thickness across this obduction zone where the overthrusting of Bahamas platform by Cuban island arc occurs. Another remarkable change of the crustal thickness occurs across Cauto-Nipe fault (CNF) (Figure 1). Otero et al. (1998) consider this fault as a divide between transitional and oceanic crust.

The characterization of the crust is, so far, mainly based on seismic refraction methods combined with gravimetric data, deep drilling and satellite photographs (Shcherbakova et al., 1978; Bovenko et al., 1982; Bush and Shcherbakova, 1986). Moreno (2003) uses teleseismic recordings of the seismological network of Cuba to estimate the crustal structure at the seismic stations, by means of the receiver functions technique. Considering the availability of surfaces wave dispersion data obtained for the Caribbean region (Gonzalez et al., 2007) we use both receiver functions and surfaces wave dispersion to constrain shear wave velocities at seismic stations and compare the new results with previous studies.

Joint inversion procedure

Receiver functions are time-series computed from three-component body-wave seismograms and sensitive to the earth structure near the receiver. They are composed by P- to S-wave or S- to P-wave conversions that reverberate within the structure below the seismic station. These converted waves are isolated by deconvolving the vertical component of a teleseismic P-wave record from its radial component (Langston, 1979; Ammon et al., 1990; Ammon, 1991). Surface waves arise from the presence (boundary conditions) of the stress free surface of the Earth's and, in presence of layering, they are dispersed. They provide valuable information on the absolute S-wave velocity (V_s) but are relatively insensitive to sharp vertical velocity contrasts. On the other hand, receiver functions are sensitive to S-wave velocity contrasts, which give rise to converted phases, but allows for substantial trade-off between the depth and velocity above an impedance change (Ammon et al., 1990). Combining both kinds of signals in a joint inversion bridges the resolution gaps associated with each individual data set (Ozalaybey et al., 1997; Julià et al., 2000, 2003, 2005; Gök et al., 2008).

The joint inversion of receiver function and surface wave dispersion follows the approach described in Julia et al. (2000). The use of the linearized inversion procedure is fully justified since, for each

station, we use as starting models all those consistent with the non-linear inversion of surface waves (Gonzalez et al., 2007), and can be described by the following system of equations:

$$\begin{bmatrix} pDs \\ qDr \\ \sigma\Delta \\ W \end{bmatrix} \vec{X} = \begin{bmatrix} p\vec{R}s \\ q\vec{R}r \\ 0 \\ W\vec{X}a \end{bmatrix} + \begin{bmatrix} pDs \\ qDr \\ 0 \\ 0 \end{bmatrix} \vec{X}o$$

where Ds and Dr are the partial derivative matrices for the dispersion measurements and the receiver function estimate, respectively; $\vec{R}s$ and $\vec{R}r$ are the corresponding vectors of residual, $\vec{X}$ is the vector of the fixed-thickness layers velocity model, $\vec{X}o$ is the starting model, Δ is a matrix that constructs the second order difference of the model $\vec{X}$.

The factor p = 1-q, is the influence parameter that controls the relative importance of receiver function and dispersion values. In particular, if p=0 only the receiver function data are used and if p=1 only the dispersion data are used. The damping factor σ balances the trade-off between data fitting and model smoothness, W is a diagonal matrix of weights to the vector $\vec{X}a$, which contains the *a priori* predefined velocity values.

Data preparation

We compute the receiver functions for 24 earthquakes (Table 1) recorded at eight seismic stations of the National Seismological Network of Cuba (Figure 1 and Table 2). The seismic stations are operating at a dynamic range of 96 db, digitizing at 100 samples per second in the 0.05 Hz to 40 Hz frequency band (Moreno, 2002). Several new data are added to a selection of the receiver function determined by Moreno (2003) - few of them have been rejected because they did not have a good signal to noise ratio. The preparation of data has been done with the SAC software (Goldstein, 1999) and the receiver functions have been computated using the Gaussian filters of 0.5, 1.0 and 2.5 Hz, with Ligorría and Ammon (1999) procedure, which uses the iterative time-domain deconvolution technique.

The dispersion relations obtained by Gonzalez et al. (2007), in the period range from 10 s to 40 s, have been extended using the group velocity tomographic results of Vdovin et al. (1999) ranging from 50 s to 150 s. The experimental errors of these measurements for each period vary between 0.06 km/s and 0.09 km/s.

Inversion procedure

The drawbacks intrinsic in the linearization of a non-linear problem are minimized considering as starting model of the linear procedure, for each cell where the stations are located, the set of models determined by the non-linear inversion of the dispersion curves of the Caribbean region, made by Gonzalez et al. (2007).

The joint inversion procedure builds upon two existing programs: SURF (Herrmann, 1987) for surface-wave dispersion inversion and BODY (Ammon et al., 1990) for receiver function inversion. Julia et al. (2000) developed the program JOINT to connect these procedures. All these programs are accessible in the software package Computer Programs in Seismology (Herrmann and Ammon, 2002).

Considering the characteristics of our dataset, which have poorly constrained features (small amplitude arrivals) after 35 s in the receiver functions, and our interest for mapping crustal and upper mantle layers rather than lower mantle, we parametrized layers down to the upper mantle zone. For this reason we limit the joint inversion to the first 40 s of the receiver function. In the inversion algorithm the damping factor is an important parameter because it balances the trade-off between resolution and stability (Julia et al., 2000). For each iteration, we perform the joint inversion with: (a) damping factor σ=0.5, (b) none *a priori* information and (c) influence parameter p=0.2. The last

choice gives more weight to the receiver function than to the dispersion data that define the initial models. All the layers of the initial models are inverted, but, considering the relatively poor resolution of the dispersion values at 10 s or greater for the uppermost layers, the weights for the inversion in the upper (sedimentary) layers are fixed between 0.1 and 0.8 to be consistent with our dataset resolution.

For each initial model, each iteration of the linearized inversion is controlled by a misfit function. The misfit function controls the variation of the average of the percent of fits between the experimental and the theoretical receiver functions generated by the inversion for all used earthquakes at the considered frequencies (see section Data preparation). The iterative process is terminated when the improvement of the misfit function from one iteration to the next is less than 0.05%. An example of the joint inversion procedure for one initial model from Gonzalez et al. (2007) is shown in figure 2.

The end model satisfies the following two criteria: (a) it is the solution with the percent of fit for receiver functions as close as possible to the average value of all percent of fit of all the solutions for the station (this criterion reduces the effects of the projection of possible systematic errors into the inverted structural model) and (b) it corresponds to a dispersion curve whose standard error with respect to observed group velocities is less than 0.045 km/s, i.e. equal to the value of r.m.s used by Gonzalez et al. (2007).

The thicknesses of the layers in the models determined by Gonzalez et al. (2007) are consistent with the resolving power of dispersion data (Panza, 1981). In order to optimize the layering (i.e. the subdivision of the physical layers) for the joint inversion, stability tests have been done: the layers resulting from the non-linear inversion have been subdivided into sub-layers with thickness equal to the "incremental step" used in the non-linear inversion, divided by 1, 1.25, 1.5 and 2. An example of the final results obtained for the four tests is illustrated in Figure 3, relative to station MOA. In general, the results of the four tests show that the final models: a) are internally consistent, b) their dispersion curves are consistent with the dispersion data (and the related experimental errors), and c) the percentage of fit for their receiver functions are similar. For this reason, in order to avoid an oversampling in the parametrization and to exploit the resolving power of the receiver functions, we use the 1.25 dividing factor in the sub-layering generation.

The solutions for the different stations that satisfy the described criteria, are shown in Figure 4, while, for each station, the results of the inversion corresponding to the chosen solution, are shown in Figures 5-11.

Results

As we could expect, the results for the joint inversion, summarized in tables 3 and 4 and shown in Figure 4, improve, with respect to the initial ones, the resolution in most of the end models and the uncertainty in V_s values is, as a rule, less than 0.4 km/s.

From West to East of the Cuban island, the model (see Figure 5) in the Soroa station (SOR), located in its western part (see Figure 1), indicates a low velocity channel in the lower crust and the Moho at around 26 km of depth, in good agreement with the earlier classification as thinned continental (transitional) crust (Tenreyro et al., 1994). A well pronounced layering is seen in the upper mantle and the lithospheric thickness is about 80 km; at a depth of 100 km, a stack of layers (approximately 50 km thick) characterized by relatively high velocities (ranging from 4.5 to 4.7 km/s) may indicate the presence of a subducted lithosphere.

The result for Manicaragua station (MGV) (see Figure 6) indicates that the crust is of accretional type and around 21 km thick, with an upper and lower crust of about 9 km and 8 km thick, respectively. The sub-Moho velocity is around 4.1 km/s for about 11 km of thickness, increasing up to 4.5 km/s at a depth of approximately 36 km, followed by a low velocity channel. The deep low velocity zone, starting at a depth of 200 km, could belong to a deep asthenosphere.

The model for Cascorro station (CCC) (see Figure 7), evidences a crust of continental type, about 26 km thick with an upper crystalline crust and a lower crust, with a thickness of 13 and 10 km, respectively. The crustal thickness is slightly smaller than the ones proposed by previous studies in the zone (e.g. Bovenko et al., 1982; Bush and Shcherbakova, 1986; Otero et al., 1998; Moreno 2003)

(see Table 5 for the comparison) but it is consistent with the classification made by Tenreyro et. al. (1994), indicating a thinned continental (transitional) crust. A low velocity channel is observed at the bottom of the crust, while a well developed low velocity channel, below by a thick lithosphere, is present in the mantle starting at a depth of 130 km.

In the eastern region of Cuba, 5 broad band stations are located where the tectonics processes are most intensive (Arango, 1996) and the Bouguer anomalies have their highest values (Cuevas et al., 2001). Las Mercedes station (LMG) is located in a zone where important gradients in Bouguer anomalies occur (Cuevas et al., 2001), close to the Cauto-Nipe system fault (CNF) (see Figure 1), where a remarkable change in the crustal thickness takes place (Bovenko et al.,1982; Bush and Shcherbakova, 1986; Otero et al., 1998). Here (see Figure 8) the Moho lies at a depth of about 21 km, in agreement with the range proposed by previous studies, and the lithosphere is about 80 km thick, value consistent with an oceanic type of structure. In the depth range between 110 km and 160 km, a stack of relatively high velocity layers is found that could be explained by the presence of a subducted lithospheric slab. This feature is present also in the other stations in the southeastern part of Cuba, like Rio Carpintero (RCC, Figure 8) and in Guantanamo (GTBY, Figure 9), indicating the presence of a subducted slab, with varying thickness, that could be explained by the underthrusting of this region by the Caribbean plate. This underthrusting could be the origin of the Santiago Deformed belt and it could be related to the north-south compression, starting at about 78°W and continuing all the way to the east along the southern Cuban margin, as described by Calais et al. (1998).

The result for the RCC station (see Figure 9) shows a thick oceanic crust with a thickness of about 18 km, in agreement with the classification made by Tenreyro et al., (1994), and fully consistent with the previous refraction seismic profiles (e.g. Bovenko et al. (1982); Otero et al. (1998) and Moreno (2003)). The lithospheric thickness is about 74 km, that is, a typical value for a relatively young oceanic lithosphere (e.g. Panza, 1980) while at a depth between 130 and 210 km the possible subducted lithospheric slab is present, i.e. at a larger depth than in station LMG.

The GTBY station (see Figure 10), located 80 km to the east of RCC also shows an oceanic type of crust, with a Moho about 18 km deep and a lithospheric thickness of about 75 km. A low velocity channel is present in the upper mantle at a depth of 40 km while the structure at a depth between 90 and 140 km is consistent with the presence of a subducted slab.

Figure 11 shows the result for the MOA station, where the crust is 27 km thick, in agreement with the previous study by Moreno (2003). This structure could be corresponding to an accretionary type of crust related to the presence of a compressional deformation between the Bahamas platform and the Cuban Island arc in the north coast of Cuba (Moreno, 2002). The lithosphere is about 130 km thick, while there is no clear evidence of a subducted slab.

At the easternmost part of Cuba, and at a distance of 80 km from MOA, the Maisí station (MAS) (see Figure 12) sits on a crust that is about 27 km thick and with a well pronounced low velocity channel in its upper part. This type of crust seems to be of accretionary type as well and it could be related with the compressional deformation between the Bahamas platform and the Cuban Island (Moreno, 2002). As for the MOA station, the lithosphere is about 130 km thick, and there is no clear evidence of a subducted slab.

The models obtained in this study for MOA and MAS stations are different with respect to the ones reported in earlier studies (e.g. see Table 5). Otero et al. (1998), using refraction seismic profiles and gravity data, classified the crust in Cuba in three zones: (1) a thick transitional crust (> 30 km), (2) a thin transitional crust (20 – 30 km) and (3) an oceanic crust (< 20 km). They suggest, by extrapolation from the available models, that the stations MOA and MAS are located in an oceanic crust; however, there is no seismic profile close to this area to support their hypothesis. Our results are well consistent with Moreno (2003) findings, who assigned to these sites a crustal thickness of about 29 and 24 km, respectively.

Conclusions

The joint inversion of dispersion curves and receiver functions, performed for all the broadband stations in Cuba, allows to get a relatively fine structure in most of the end models for the crust and upper mantle structure in the Cuban region. Some important features of the lithosphere and asthenosphere, including the Moho depth, the lithosphere-asthenosphere transition zone and the possible presence of subducted slabs, have been delineated below the seismic stations in Cuba. The models about the crustal thickness are mostly consistent with previous studies. New models are obtained in correspondence of MOA and MAS stations, which are more consistent with an accretional type of crust than with the oceanic type crust proposed in previous studies (mostly by extrapolation of shallow seismic profiles). For the stations RCC and GTBY the crustal and lithospheric thickness is fully consistent with an oceanic type of crust, while below the stations CCC and MGV, that are in the middle of Cuban island, the lithospheric thickness reaches values larger than 130 km. The models at the stations LMG, RCC, GTBY and SOR indicate the presence of a lithospheric slab, possibly belonging to the Caribbean plate. The subduction could be explained as the (present or past) result of the north-south compression between the Caribbean plate and the Cuba Island.

Acknowledgments

The authors are grateful to the National Seismological Service of Cuba which provided the data used in this study. The present work is done with the financial support of the Associateship Scheme, TRIL and SAND Groups of the Abdus Salam International Centre for Theoretical Physics, the Ministry of Science, Technology and Environment of Cuba, and the Italian Programma Nazionale di Ricerche in Antartide (PNRA) 2004-2006, project 2.7–2.8 (“Sismologia a larga banda nella regione del Mare di Scotia e suo utilizzo per lo studio della geodinamica della litosfera”). We thank the staff of the Department of Geosciences from the University of Trieste, for their support with software and hardware facilities.

References

Ammon, C.J., Randall, G.E. and Zandt, G., 1990, On the nonuniqueness of receiver function inversions, *J. Geophys. Res.* **95**, 15303–15318.

Ammon, C.J., 1991, The isolation of receiver effects from teleseismic P waveforms, *Bull. Seism. Soc. Am.* **81**, 2504–2510.

Arango, E. D. (1996): Geodinámica de la región de Santiago de Cuba en el límite de las placas de Norteamérica y el Caribe. Tesis de maestría. Instituto Politécnico Nacional de México. Fondos del Centro Nacional de Investigaciones Sismológicas. Santiago de Cuba, 110p.

Bovenko, V.G., Shcherbakova, B.E. and Hernández, H., 1982, Novyye geofizicheskiye dannyye o glubinnour stroyenii vostochnoy kuby (New geophysical data on the deep structure of eastern Cuba), Sovetskaya Geologiya 9, 101–109; translation in International *Geology Review* **24**, 1155–1162.

Bush, V.A. and Shcherbakova I.N., 1986, New Data on the Deep Tectonics of Cuba, *Geotectonics* **20**, 192–203.

Calais, E., Perrot, J., and Mercier de Lépinay, B., 1998, Strike-slip tectonics and seismicity along the northern Caribbean plate boundary from Cuba to Hispaniola, *in* Dolan, J. F., and Mann, P., eds., Active Strike-Slip and Collisional Tectonics of the Northern Caribbean Plate Boundary Zone: Boulder, Colorado,Geological Society of America Special Paper 326.

Cuevas, J.L, Diaz, L.A., and Polo, B. 2001. Regionalización gravimétrica en el Caribe Centro Occidental (I): Nuevos mapas de anomalías de Bouguer total y aire libre de Cuba a escala 1: 500 000. Memorias de GEOMIN 2001. GF, 93-104.

Draper, G. and Barros, J.A., 1994, Cuba (chapter 4), In: *Caribbean Geology: An Introduction*, U.W.I. Publishers' Association, Kingston, pp. 65–85.

Goldstein, P., 1999, SAC User's Manual, Lawrence Livermore Laboratory, University of California.

Gonzalez, O., Alvarez L., Guidarelli M. and Panza G.F., 2007, Crust and Upper Mantle Structure in the Caribbean Region by Group Velocity Tomography and Regionalization, *Pure appl. geophys.* **164**, 1985-2007.

Gök, R., Mahdi, H., Al-Shukri, H., and Rodgers, A.J., 2008, Crustal structure of Iraq from receiver functions and surface wave dispersion: implications for understanding the deformation history of the Arabian-Eurasian collision, *Geophys. J. Int.*, **172**, 1179-1187

Herrmann, R.B., 1987, *Computer Programs in Seismology*, Saint Louis University, St Louis, MO.

Herrmann, R.B. and Ammon C.J., 2002, *Computer Programs in Seismology: Surface waves, Receiver functions and Crustal structure*, Version 3.20, Saint Louis University, St Louis, 110 pp.

Julia, J., Ammon, C.J., Herrmann, R.B., and Correig, A.M., 2000, Joint inversion of receiver functions and surface-wave dispersion observations, *Geophys. J. Int.*, **143**, 99-112.

Julia, J., Ammon, C.J., and Herrmann R.B., 2003, Lithospheric structure of the Arabian Shield from the joint inversion of receiver functions and surface-wave group velocities, *Tectonophysics*, **371**, 1-21.

Julia J., Ammon, C.J. and Nyblade A.A., 2005, Evidence for mafic lower crust in Tanzania, East Africa, from joint inversion of receiver functions and Rayleigh wave dispersion velocities, *Geophys. J. Int.*, **162**, 555-569.

Langston, C.A., 1979, Structure under Mount Rainier, Washington, inferred from teleseismic body waves, *J. Geophys. Res.* **84**, 4749–4762.

Ligorría, J. P., and C. J. Ammon (1999). Iterative deconvolution of teleseismic seismograms and receiver function estimation, *Bull. Seism. Soc. Am.*, 89, 1395-1400.

Makarov, V.I., 1986, The Neotectonics of Eastern Cuba. Part One. General Description. Northern and Central Districts, *Geotectonics*, **20**, 515–523.

Moreno, B., 2002. The new Cuban Seismograph Network, *Seism. Res. Lett.* **73**, 505–518.

Moreno, B., Grandison M., and Atakan K., 2002, Crustal velocity model along the southern Cuba margin: implications for the tectonic regime at an active plate boundary, *Geophys. J. Int.*, **151**, 632-645.

Moreno, B., 2003, The crustal structure of Cuba derived from Receiver Function Analysis, *Journal of Seismology*, **7**, 359-375.

Otero, R., Prol, J.L., Tenreyro, R. and Arriaza, G.L., 1998, Caracteristicas de la corteza terrestre de Cuba y su plataforma marina (Characteristics of the Earth's crust in Cuba and its marine platform), *Mineria y Geologia* **15**, 31–35.

Ozalaybey, S., Savage, M.K., Sheehan, A.F., Louie, J.N., and Brune, J.N., 1997, Shear-wave velocity structure in the northern basin and range province from the combined analysis of receiver functions and surface waves, *Bull. Seism. Soc. Am.*, **87**, 183-189.

Panza, G.F., (1980). Evolution of the Earth's lithosphere. NATO Adv. Stud. Inst. Newcastle, 1979. In: Mechanisms of Continental Drift and Plate Tectonics. Ed.: Davies,P.A. and Runcorn, S.K., Academic Press, pp. 75-87.

Panza, G.F., The Resolving power of seismic surface waves with respect to crust and upper mantle structural models, In The Solution of the Inverse Problem in Geophysical Interpretation (Cassinis, R. ed.) pp. 39–77.(Plenum Publ. Corp. 1981)

Pardo, G., 1975, Geology of Cuba (chapter 13), In: Nairn, A.E.M. nd Stehli, F.G. (eds), *The Ocean Basins and Margins*, Vol. **3**, pp. 553–615, Plenum Publishing, New York.

Pushcharovskiy, Y.M., 1979, The tectonics and geodynamics of the Caribbean region, *Tektonicheskoye razvitiye zemnoy kory i razlomy* (Tectonic Evolution of the Earth's Crust and Faults), Moscow, Nauka, pp. 124–132.

Shcherbakova, B.E., Bovenko, V.G. and Hernández, H., 1978, Stroyeniye zemnoy kory Zapadnoy Kuby (Crustal structure in West Cuba), *Sovetskaya Geologya*, **8**, 138–143; translation in *International Geology Review*, **20**, 1125–1130.

Tenreyro, R., López, J. G., Echevarría, G., Alvarez, J., Sánchez, J. R. (1994). Geologic Evolution and Structural Geology of Cuba. Abstracts AAPG Annual Meeting, June 12- 15. Denver. Colorado.

Vdovin, O., Rial, J.A., Levshin, A.L. and Ritzwoller, M. H. (1999). "Group-velocity Tomography of South America and the Surrounding Oceans". Geophys. J. Int., 136, 324-340.

Table 1. List of the teleseismic records used in the receiver function computation.

From previous study (Moreno, 2003)						From this study					
Date	**Time**	**Lat.**	**Lon.**	**Dep.**	**Ms**	**Date**	**Time**	**Lat.**	**Lon.**	**Dep.**	**Ms**
19980403	2201	-8.15	-74.24	164	6.6	20040503	0436	-37.70	-73.41	21	6.6
19980522	0448	-17.73	-65.43	24	6.6	20050521	0511	-3.29	-80.99	39	6.4
19980903	1737	-29.45	-71.71	27	6.6	20050613	2244	-19.90	-69.13	110	7.9
20010626	0418	-17.75	-71.65	24	6.7	20050926	0155	-5.68	-76.40	115	7.5
20010705	1353	-16.09	-73.99	62	6.6	20051117	1926	-22.32	-67.89	162	6.8
20010707	0938	-17.54	-72.08	33	7.6	20060430	1917	-26.99	-70.79	7	6.4
20010724	0500	-19.45	-69.25	33	6.4	20061020	1048	-13.43	-76.57	33	6.5
20020328	0456	-21.66	-68.33	125	6.5	20070815	2340	-13.32	-76.51	40	7.5
20020401	1959	-29.67	-71.38	71	6.4	20071115	1503	-22.87	-70.41	27	6.1
20020418	1608	-27.53	-70.59	62	6.7	20071216	0809	-22.56	-69.98	55	6.7
20030620	1330	-30.61	-71.64	33	6.8	20080208	0938	10.67	-41.90	9	6.9
20031222	1915	35.71	-121.10	7	6.6	20080523	1935	7.31	-34.9	8	6.5
						20080910	1308	8.09	-38.72	10	6.4

Table 2. Broadband seismic stations used in this study.

Station	Latitude (°N)	Longitude (°W)	Elevation (m)
MAS	20.18	74.23	350
MOA	20.66	74.96	50
RCC	19.99	75.70	100
LMG	20.06	77.00	167
CAS	21.19	77.42	66
MCG	22.11	79.98	100
SOR	22.78	83.01	206
GTBY	19.93	75.11	19.93

Table 3. Vs velocity models for each seismological station derived from the joint inversion.

SOR		MGV		CCC		LMG	
Thick (km)	Vs (km/sec)	Thick (km)	Vs (km/sec)	Thick (km)	Vs (km/sec)	Thick (km)	Vs (km/sec)
0.6	2.13	4	2.98	1	1.98	1.5	1.82
3.2	2.86	3.8	2.96	2.5	2.87	2.6	3.09
3.2	2.91	5	3.02	7	3.02	2	3.44
3.2	3.08	2	3.52	5	3.26	2	2.81
5.8	3.57	2	3.78	2	3.82	3	3.19
3.2	3.82	2	3.85	2	3.92	4.8	3.42
3.2	3.53	2	3.65	2	3.92	5.2	3.69
3.2	3.87	2.7	4.04	2	3.80	18	4.31
3.2	4.18	2.7	3.99	2	3.62	8	4.58
5.2	4.11	2.7	4.07	6.4	4.16	16	4.69
8	4.48	2.7	4.18	9.6	4.27	13	4.49
12	4.64	4.2	4.26	24	4.50	32	4.3
25	4.56	6.6	4.45	16	4.56	32	4.75
16	4.35	3.3	4.31	16	4.53	16	4.62
16	4.7	3.3	4.26	38	4.52	16	4.28
32	4.63	3.3	4.39	40	4.38	32	4.11
32	4.44	70	4.48	40	4.25	16	4.2
32	4.46	80.1	4.55	40	4.54	16	4.39
32	4.27	33.2	4.31	40	4.56	20	4.65
32	4.61	26.7	4.33	54.5	4.54	32	4.95
32	4.69	26.7	4.45	17	4.90	16	4.64
47	4.85	26.7	4.57			16	4.65
17	4.9	34.1	4.67			29.9	4.81
50	4.9	67	4.90			17	4.9

RCC		GTBY		MOA		MAS	
Thick (km)	Vs (km/sec)	Thick (km)	Vs (km/sec)	Thick (km)	Vs (km/sec)	Thick (km)	Vs (km/sec)
1	1.25	1	1.41	0.6	1.75	0.6	1.84
1.7	2.74	1.7	2.90	3.2	3.06	3.2	3.26
8	3.37	15	3.32	3.2	2.97	3.2	3.07
4	3.18	6	4.05	3.2	2.89	3.2	2.98
3	3.35	8	4.15	3.2	3.25	3.2	3.15
10	4.31	2	4.25	3.2	3.56	3.2	3.47
4	4.14	4	4.40	3.2	3.67	3.2	3.65
2	4.20	2	4.30	3.5	3.92	3.5	3.81
11	4.28	5	4.18	4	3.63	4	3.57
24	4.71	9.6	4.60	8	4.28	8	4.34
4.8	4.59	9.6	4.75	8	4.40	8	4.30
35.2	4.46	4.8	4.84	8	4.44	8	4.33
12	4.19	4.8	4.63	8	4.65	8	4.53
12	4.33	4.8	4.37	23	4.48	23	4.53
12	4.49	6.4	4.23	50	4.60	20	4.66
20	4.57	4.8	4.36	60	4.33	32	4.47
16	4.58	46.2	4.58	32	4.49	32	4.37
16	4.68	94	4.31	32	4.41	32	4.43
16	4.49	16	4.59	32	4.62	54	4.46
16	4.19	16	4.67	61.7	4.73	32	4.59
26	4.04	32	4.81	17	4.90	32	4.55
16	4.55	16	4.67	50	4.90	33.7	4.88
16	4.71	16	4.50			17	4.90
16	4.83	24.3	4.70			50	4.90
16	4.98	17	4.90				

Table 4. Crust and lithosphere thickness and range of depth for the subducted slab (where present) below the seismic stations in Cuba.

Station	SOR	MGV	CCC	LMG	RCC	GTMO	MOA	MAS
Crustal thickness (km)	26	21	26	21	18	18	27	27
Lithospheric thickness (km)	79	202	135	76	74	74	132	134
Range of depth for subducted slab (km)	95 - 145			108 - 156	132 - 213	90 - 136		

Table 5. Comparison of crustal thickness at seismic stations derived from different studies. Question mark indicates probable thickness extrapolated from relatively distant seismic cross sections.

Station	Bovenko et al., 1982	Bush and Shcherbakova, 1986	Otero et al, 1998	Moreno, 2003	This study
MAS	-	-	< 20 km	24 km	27 km
MOA	-	-	< 20 km	29 km	27 km
RCC	18 km (?)	-	< 20 km	18 km	18 km
LMG	21 km (?)	17-24 km (?)	< 20 km	19 km	21 km
CCC	32 km (?)	35 km (?)	> 30 km	31 km	26 km
MGV	-	17-24 km (?)	20-30 km	24 km	21 km
SOR	-	30 km (?)	20-30 km	27 km	26 km
GTBY	-	-	-	-	18 km

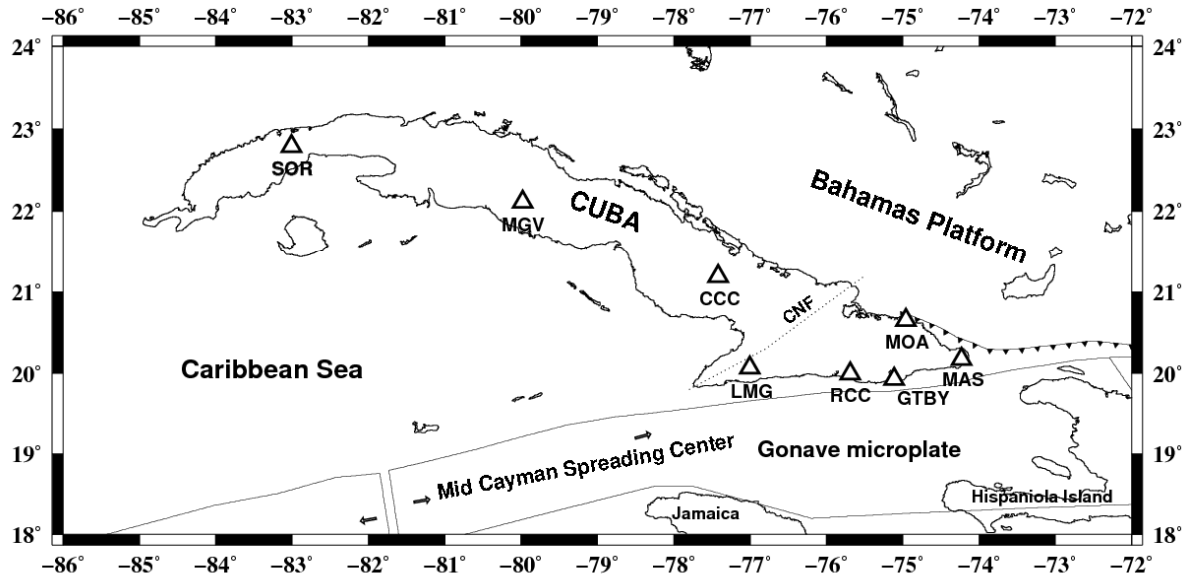

Figure 1. Location of seismic stations (modified from Moreno, 2003). Dashed lines represent the Cauto-Nipe fault (CNF).

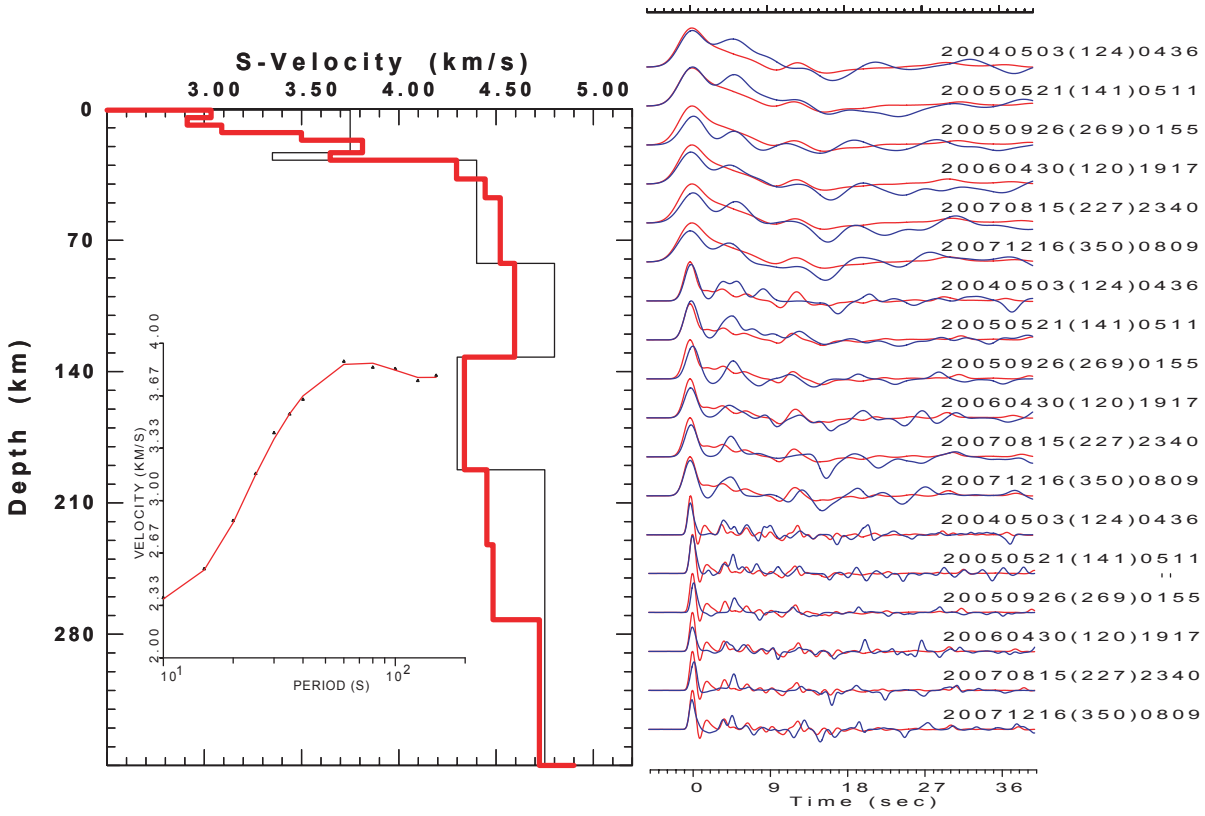

Figure 2. Example of joint inversion for MOA station; the initial input model is one of the solutions obtained by Gonzalez, (2007). Thick red line in the left plot corresponds to the chosen solution while numbers in receiver functions correspond to origin time of the seismic event.

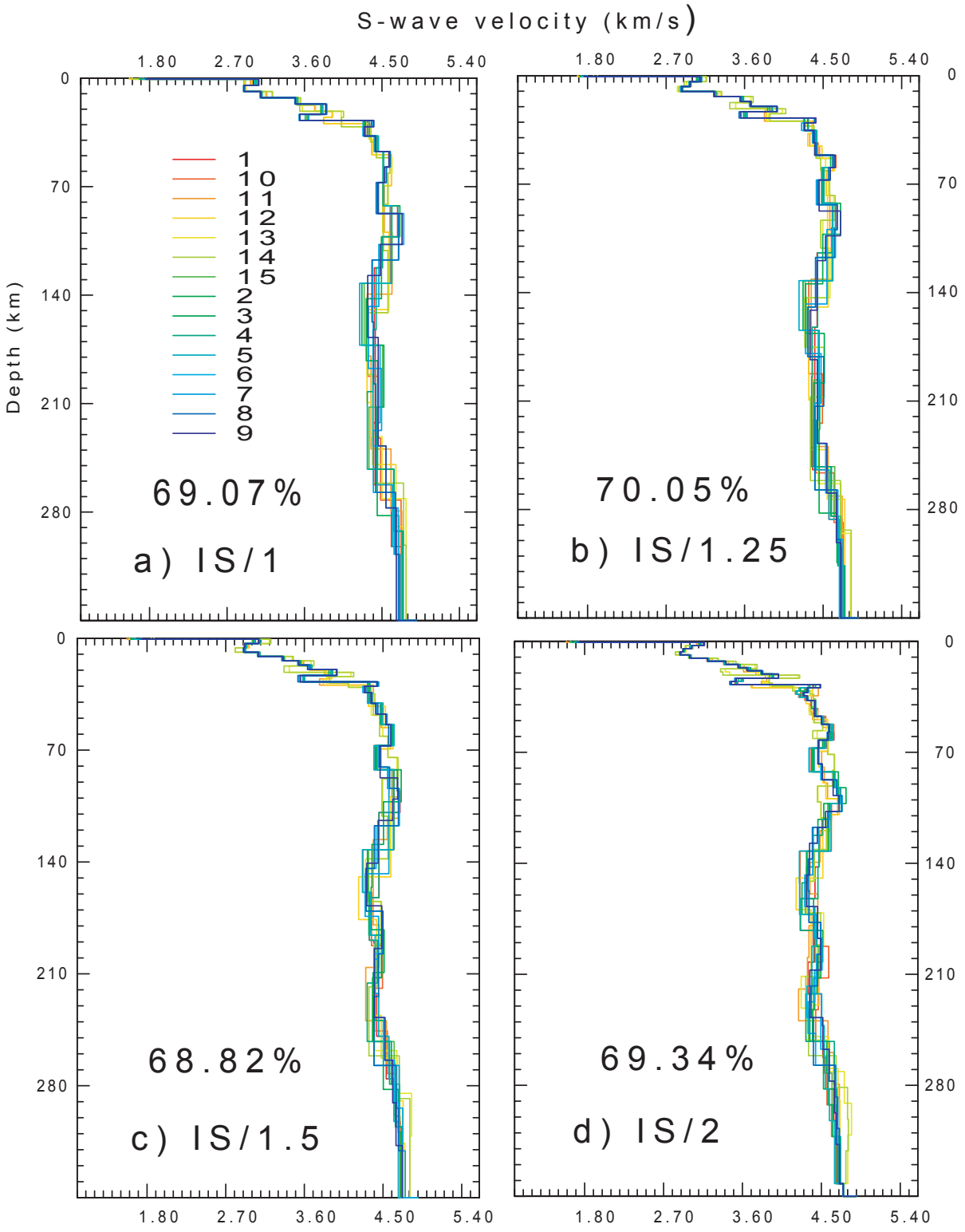

Figure 3. Final results obtained for the four stability tests performed at station MOA. The starting thickness of the layers in the initial models (15 in total) was determined by Gonzalez et al. (2007), using in the inversion the "incremental step" (IS), calculated on the base of the resolving power of dispersion data. The initial layers were subdivided in sub-layers with thickness equal to the corresponding IS divided by 1 (a), 1.25 (b), 1.5 (c) and 2 (d). For each case, the percentage indicates the maximum value obtained for the fit (between theoretical and experimental RFs) considering all the initial models.

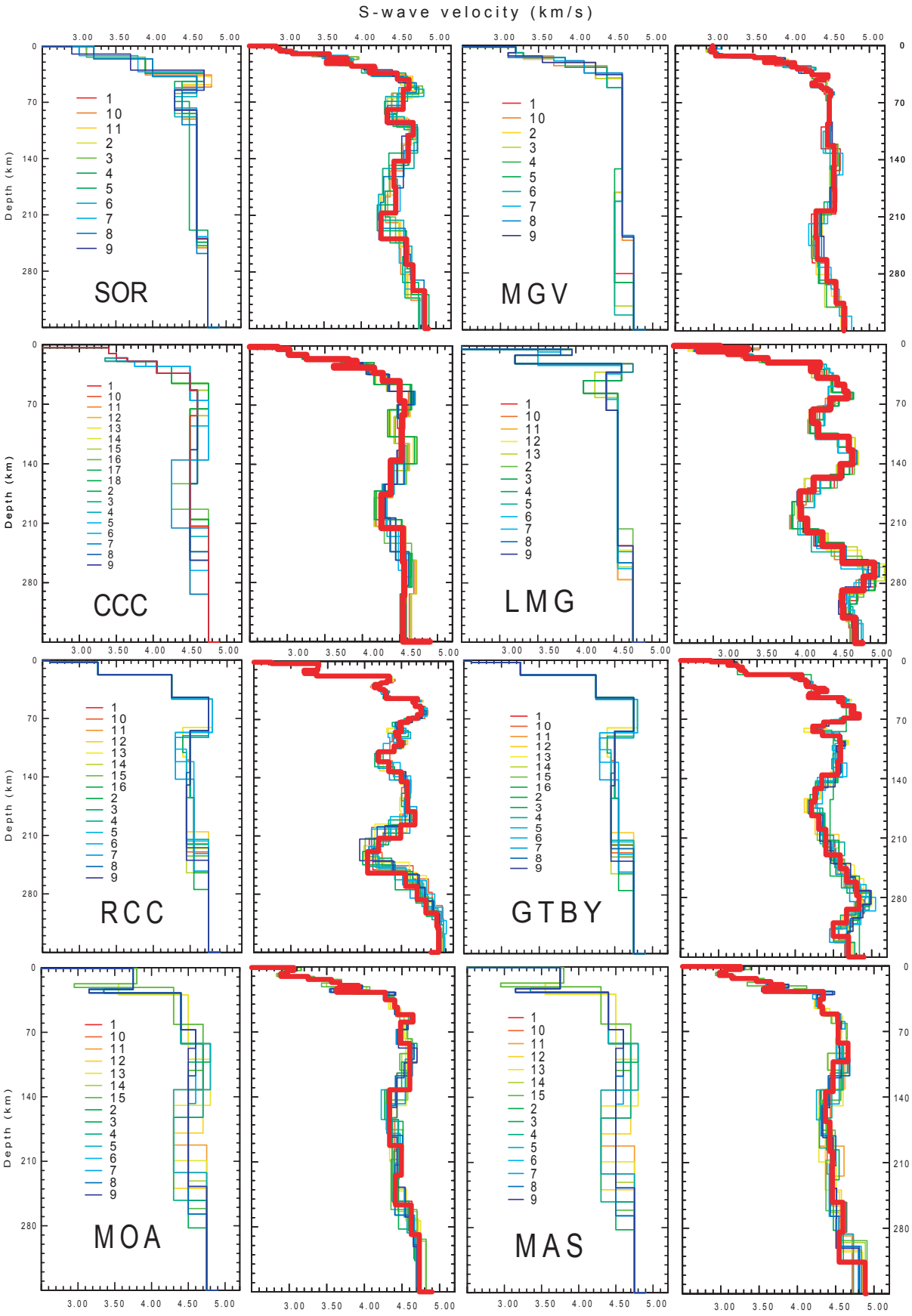

Figure 4. Initial and final models, for each considered station; thick red lines indicate the chosen solution, according to the criterion described in the text.

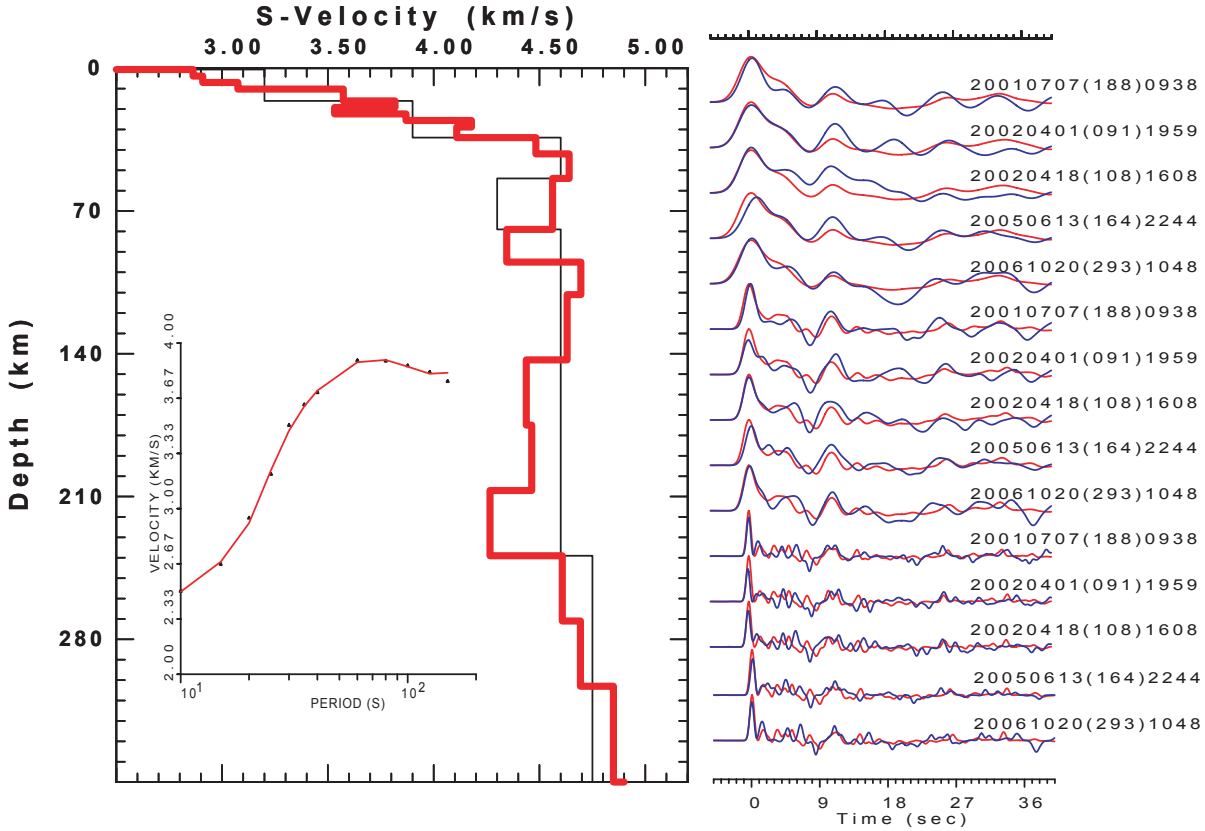

Figure 5. Chosen solution (thick red line in the left plot) for Soroa station (SOR), result of the joint inversion of RFs (using Gaussian filters at 0.5, 1.0 and 2.5 Hz) and dispersion data.

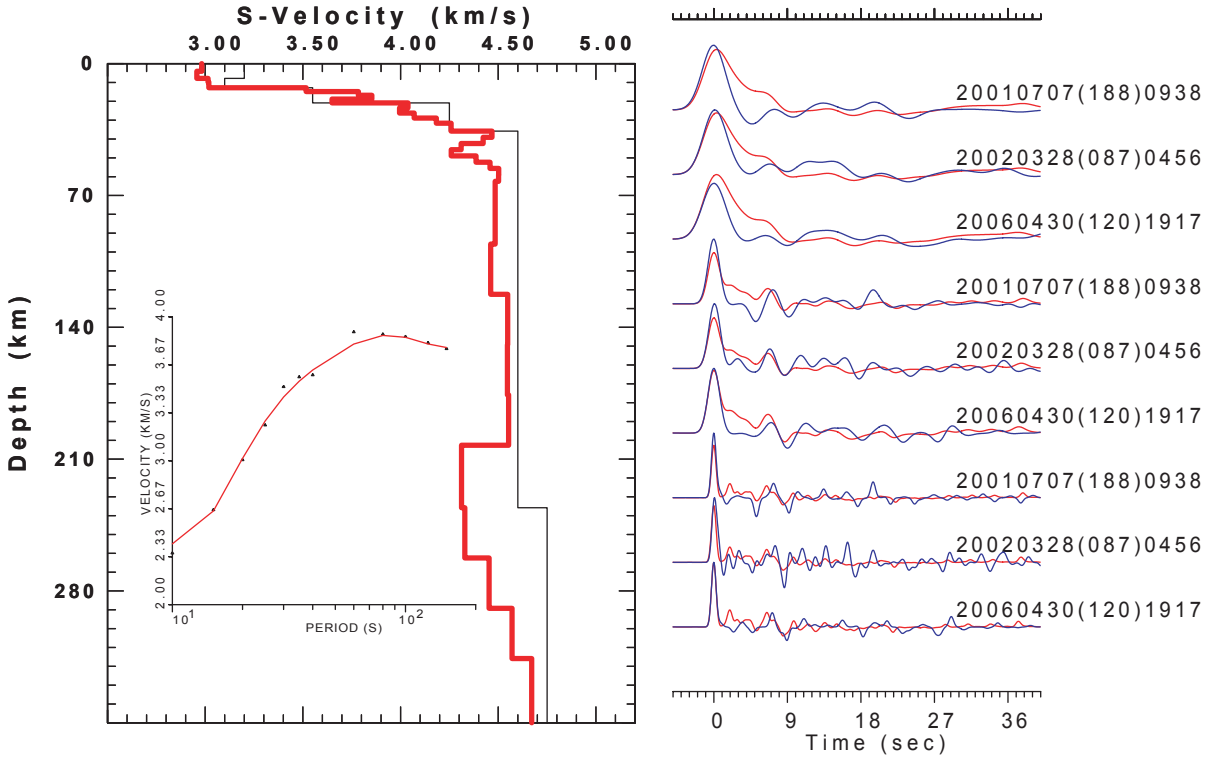

Figure 6. Chosen solution (thick red line in the left plot) for Manicaragua station (MCG), result of the joint inversion of RFs (using Gaussian filters at 0.5, 1.0 and 2.5 Hz) and dispersion data.

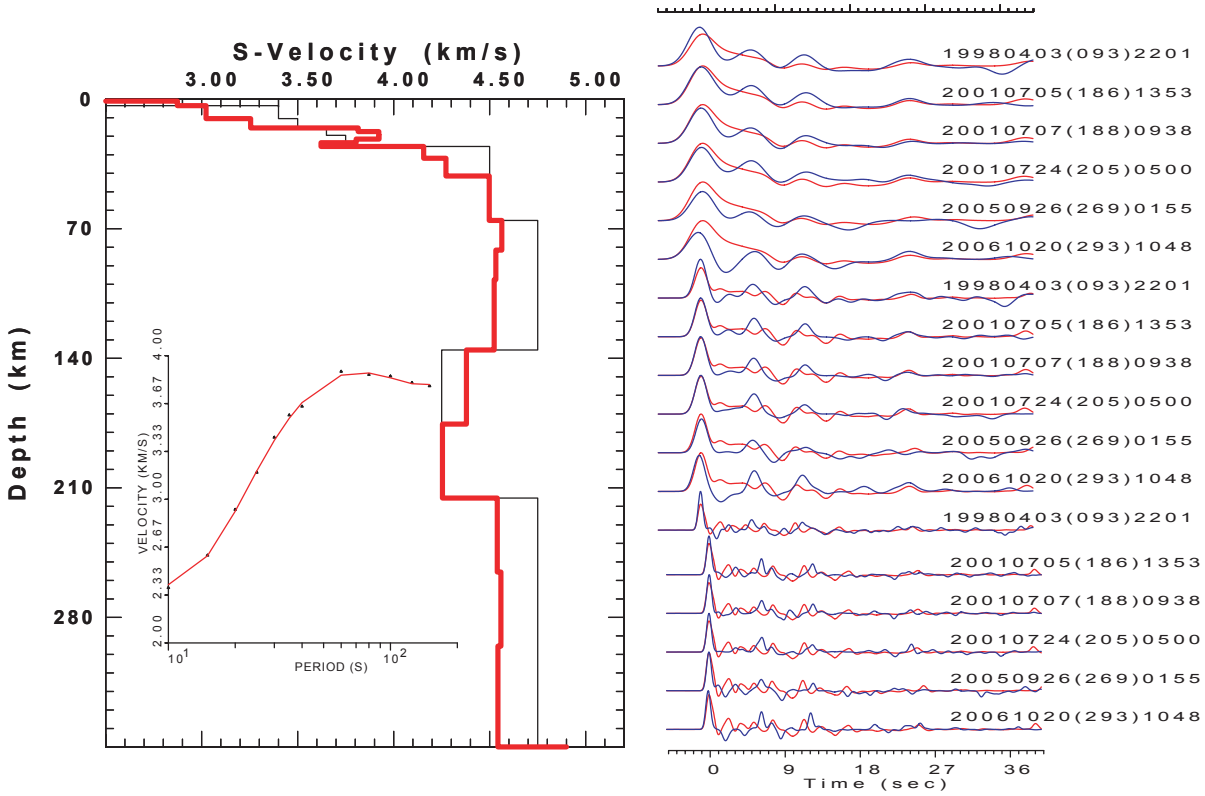

Figure 7. Chosen solution (thick red line in the left plot) for Cascorro station (CCC), result of the joint inversion of RFs (using Gaussian filters at 0.5, 1.0 and 2.5 Hz) and dispersion data.

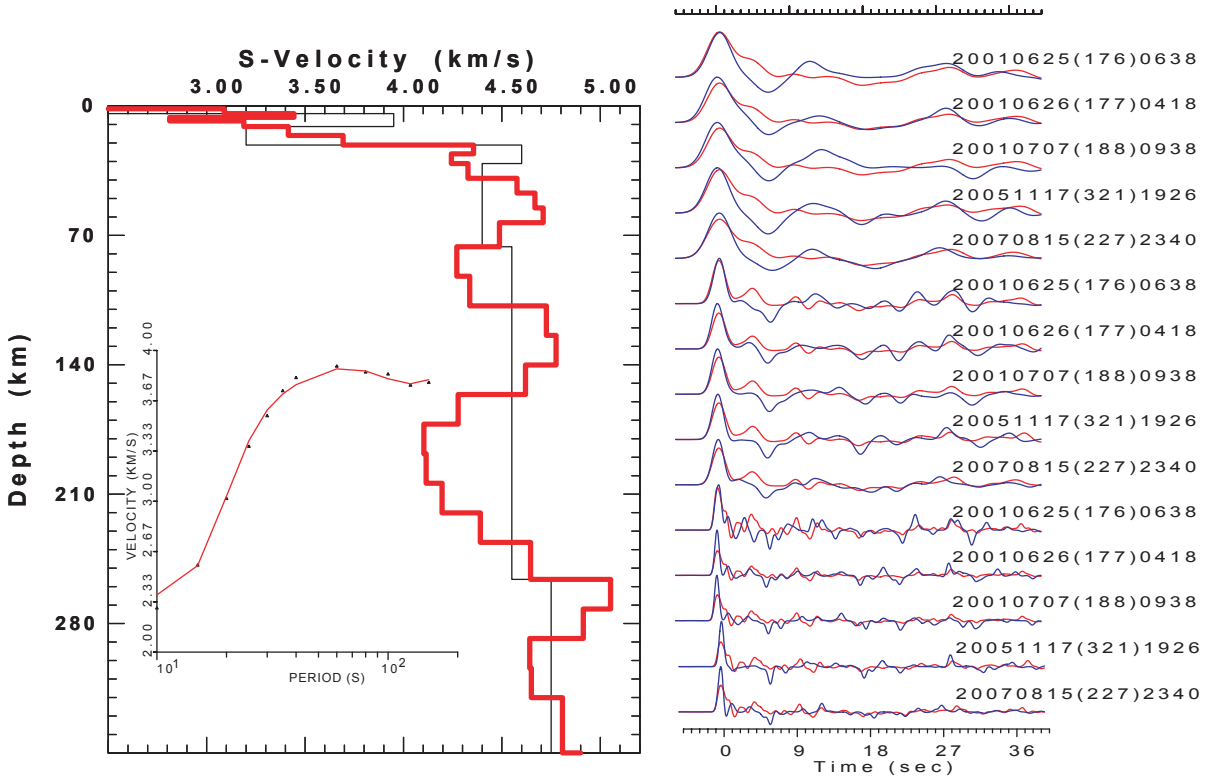

Figure 8. Chosen solution (thick red line in the left plot) for Las Mercedes station (LMG), result of the joint inversion of RFs (using Gaussian filters at 0.5, 1.0 and 2.5 Hz) and dispersion data.

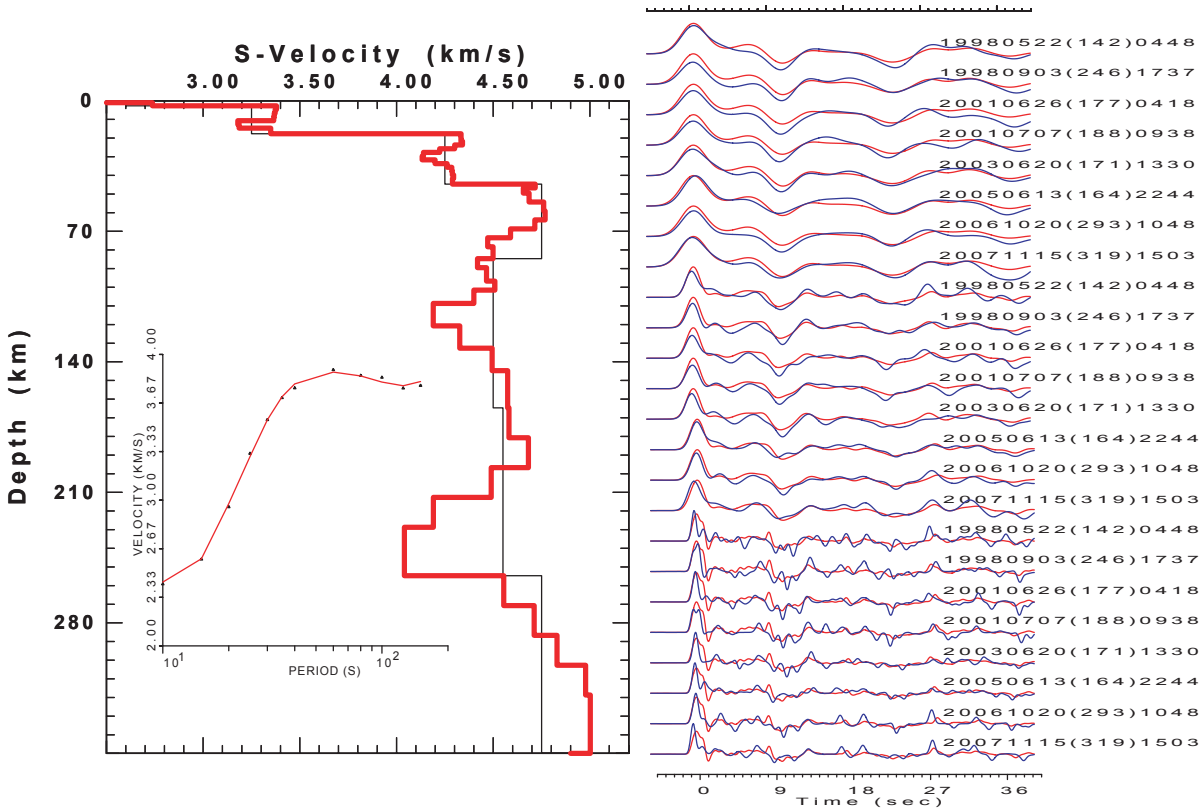

Figure 9. Chosen solution (thick red line in the left plot) for Rio Carpintero station (RCC), result of the joint inversion of RFs (using Gaussian filters at 0.5, 1.0 and 2.5 Hz) and dispersion data.

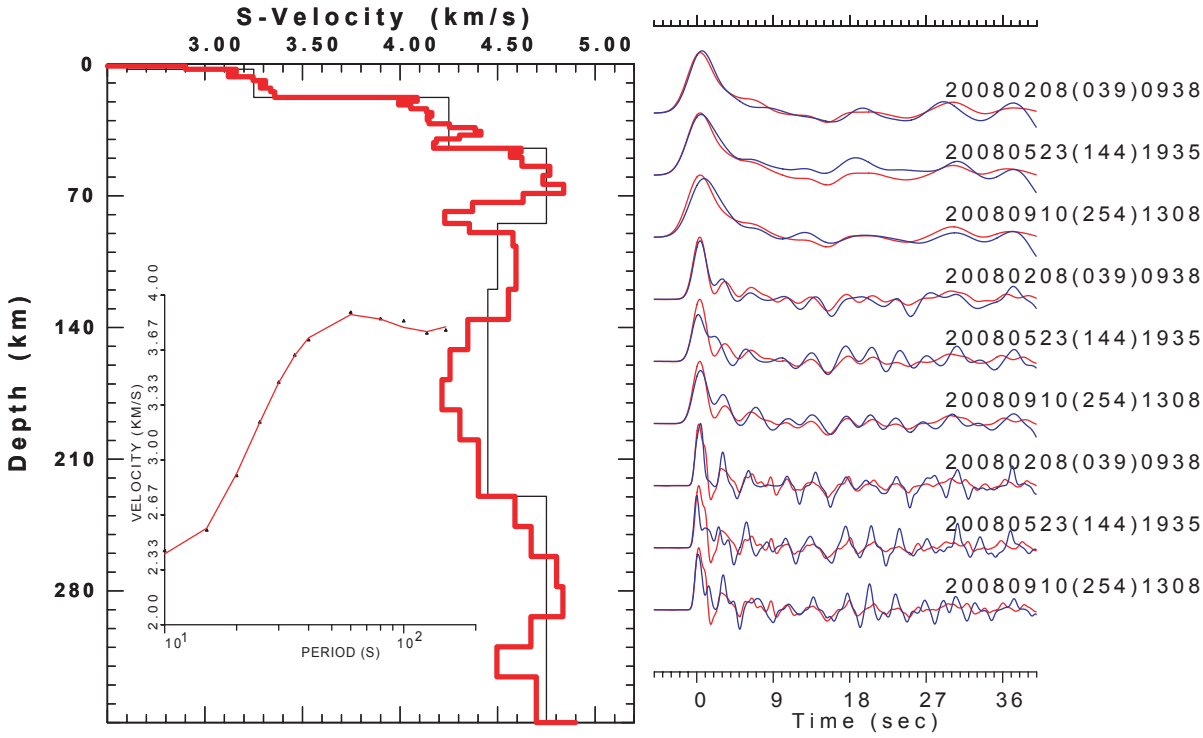

Figure 10. Chosen solution (thick red line in the left plot) for Guantanamo Bay station (GTBY), result of the joint inversion of RFs (using Gaussian filters at 0.5, 1.0 and 2.5 Hz) and dispersion data.

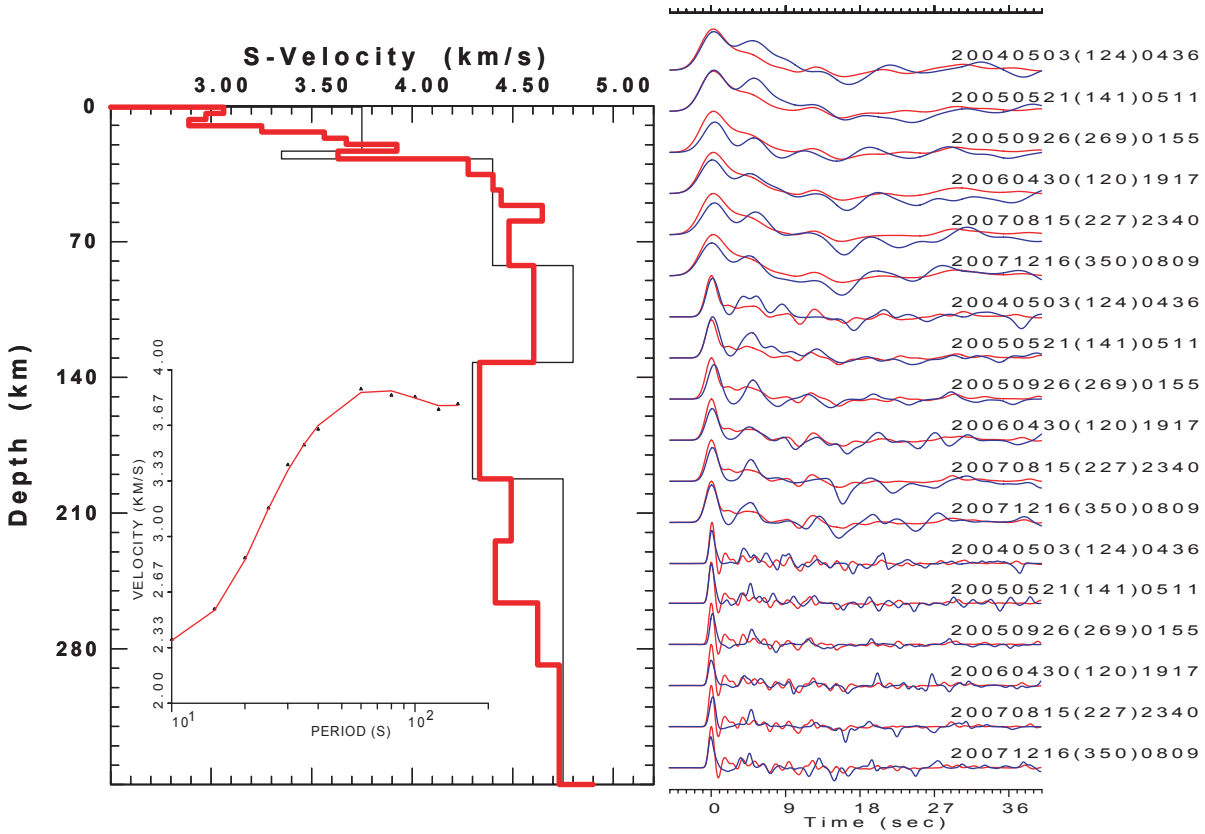

Figure 11. Chosen solution (thick red line in the left plot) for Moa station (MOA), result of the joint inversion of RFs (using Gaussian filters at 0.5, 1.0 and 2.5 Hz) and dispersion data.

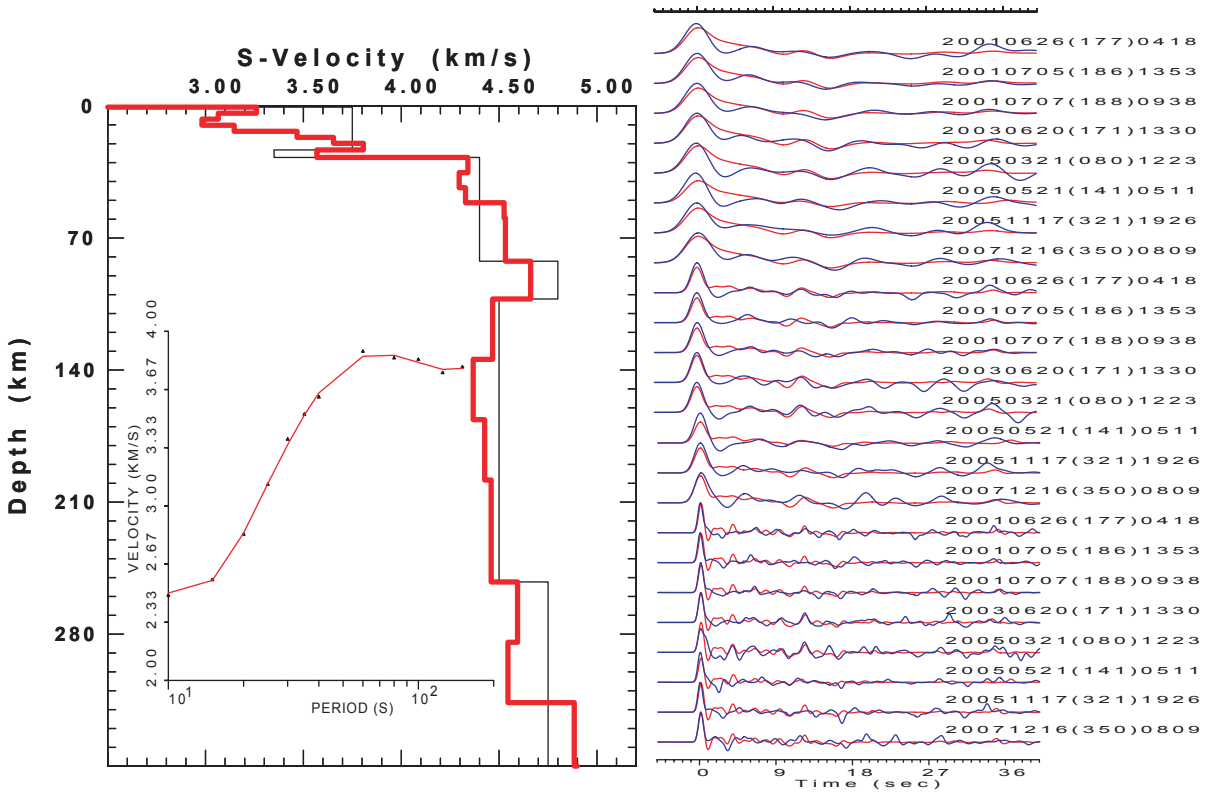

Figure 12. Chosen solution (thick red line in the left plot) for Maisí station (MAS), result of the joint inversion of RFs (using Gaussian filters at 0.5, 1.0 and 2.5 Hz) and dispersion data.